

Supporting Information for

Insights into the magmatic feeding system of the 2021 eruption at Cumbre Vieja (La Palma) inferred from gravity data modeling

Fuentsanta G. Montesinos ^{1,7*}, Sergio Sainz-Maza ^{2,7}, David Gómez-Ortiz ³, José Arnosó ^{4,7},
Isabel Blanco-Montenegro ^{5,7}, Maite Benavent ^{1,7}, Emilio Vélez ^{4,7}, Nieves Sánchez ⁶ and Tomás
Martín-Crespo ³

- ¹ Facultad de CC. Matemáticas, Universidad Complutense de Madrid, Plaza de Ciencias 3, 28040 Madrid, Spain; fuentsant@ucm.es (F.G.M.); mbena@mat.ucm.es (M.B.)
- ² Observatorio Geofísico Central (IGN), C/Alfonso XII, 3, 28014 Madrid, Spain; ssainz-maza@mitma.es
- ³ Departamento de Biología y Geología, Física y Química Inorgánica, ESCET, Universidad Rey Juan Carlos, C/Tulipán s/n, 28933 Móstoles, Madrid, Spain; david.gomez@urjc.es (D.G.-O.); tomas.martin@urjc.es (T.M.-C.)
- ⁴ Instituto de Geociencias (IGEO, CSIC-UCM), C/Doctor Severo Ochoa, 7, 28040 Madrid, Spain; jose.arnosó@csic.es (J.A.); emilio.velez@csic.es (E.V.)
- ⁵ Departamento de Física, Escuela Politécnica Superior, Universidad de Burgos, Avda. de Cantabria s/n, 09006 Burgos, Spain; iblanco@ubu.es
- ⁶ Instituto Geológico y Minero de España (IGME, CSIC), Unidad Territorial de Canarias, Alonso Alvarado, 43, 2A, 35003 Las Palmas de Gran Canaria, Spain; n.sanchez@igme.es
- ⁷ Research Group 'Geodesia', Universidad Complutense de Madrid, 28040 Madrid, Spain

* Correspondence: fuentsant@ucm.es

S1. Spatiotemporal distribution of the earthquakes that occurred in La Palma during the 2021 eruption.

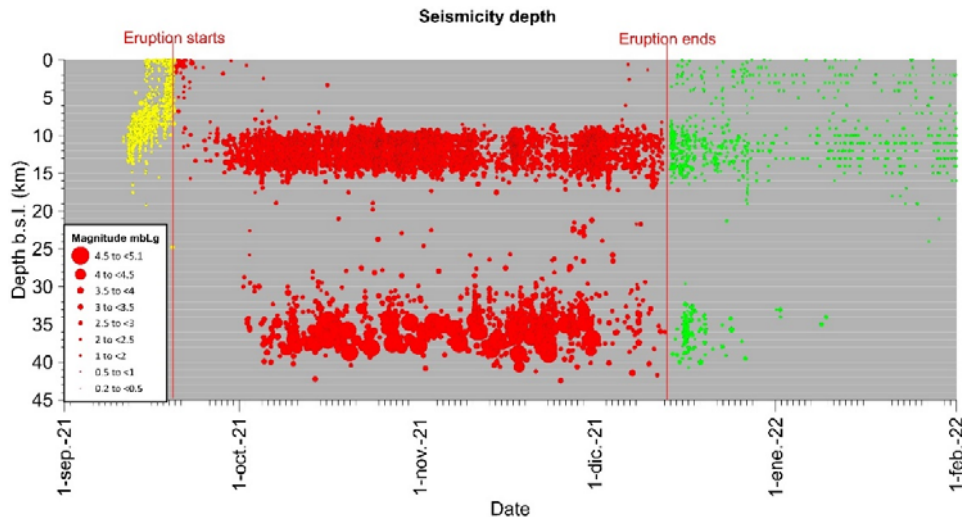


Figure S1. Time series of the volcanotectonic (VT) earthquakes associated to the Cumbre Vieja eruptive process (from September 19th to December 13th, 2021). The yellow cluster corresponds to the pre-eruptive seismicity, that occurred progressively shallower and preceding the fissure eruption. Red circles represent the co-eruptive seismicity with two different clusters located at ~11 km and ~35 km mean depths. Green circles correspond to the post-eruptive events, showing that while the occurrence of deep VT events rapidly decay

with time (almost completely vanishing from January 2022), the shallower events remain almost constant at the same mean depth (earthquake data locations provided by the Spanish National Geographic Institute (IGN), <https://www.ign.es/web/ign/portal/sis-catalogo-terremotos>).

S2. Gravity stations

Table S1. Geographic coordinates of the stations of the gravity network located on La Palma obtained from GNSS observations made during the gravity survey in January 2022.

Gravity network				
Station	Latitude (°)	Longitude (°)	Height (m)	
1. PALM_EVIR	28.6629	-17.8414	907.190	
2. Futbolpaso	28.6481	-17.8839	610.226	
3. PALM_ENIC	28.6021	-17.8804	617.437	
4. Ermisidro	28.6410	-17.7971	576.740	
5. Absebel	28.5795	-17.7745	337.116	
6. Monteluna	28.5435	-17.8114	671.425	
7. PinolaVirgen	28.5095	-17.8261	751.928	
8. PALM_EANT	28.4953	-17.8447	721.739	
9. Busmicharco	28.5349	-17.8659	767.678	
10. Pistastr1	28.6166	-17.8489	1346.546	
11. Pistastr2	28.6013	-17.8531	1337.794	
12. Busnaos	28.5877	-17.9097	25.250	
13. Losretamales	28.5105	-17.8557	746.965	
14. Canfuego	28.6012	-17.8858	552.848	
15. Cintsant	28.4869	-17.8479	633.500	

Table S2. Absolute Gravity values from the gravity network of the Spanish National Geographic Institute. These gravity values are reduced by the height of the instrument to the benchmark (available in <https://www.ign.es/web/ign/portal/grv-gravedad-absoluta>).

Absolute stations (Spanish National Geographic Institute)				
Station	Latitude (°)	Longitude (°)	Height (m)	Gravity (μGal)
PALM_EVIR	28.66296	-17.84142	907.22	979278583.
PALM_ENIC	28.60213	-17.88045	617.28	979297075.
PALM_EANT	28.49528	-17.84474	721.79	979230572.

S3. Terrain correction applied to the gravity data.

Table S3. Features of the grid used for the terrain correction around each gravity station. The terrain has been divided into several zones defined from R1 to R2 distance from the station. We used fine grids interpolated from the 5 m digital elevation model (DEM) to perform the near zone correction (1 to 50 m). In each zone, the prisms of S size represent the terrain, and E is the scale of the DEM used.

ZONE	From R1 (m)	To R2 (m)	Prisms size S (m)	DEM E (m)
1	0	10	0.2	5
2	10	50	1	5
3	50	1000	5	5
4	1000	5000	25	25
5	5000	25000	50	50
6	25000	167000	500	500

S3.1. *The method of Nettleton to calculate an approximate terrain density value*

We developed a comprehensive analysis based on the Nettleton methodology [84] to calculate the most appropriate density value to use for the terrain correction. The Nettleton procedure assumes that the statistical correlation between Bouguer anomaly and the height of the corresponding station should be minimal. This methodology is widely used in areas where rock density data are not available. In volcanic areas, however, the Nettleton's method is less effective in obtaining rock density because of successive overlapping of different lavas and volcanic products that have shaped the terrain. Thus, aiming to establish a density zonation for the island, we applied the Nettleton's method every 100 m over the onshore area. We calculated this calculation using the gravity data within a radius of 8,000 m around each point to ensure enough observations at each step, and to obtain a smooth information model. Figure S2 shows the results for La Palma island. It can be seen a wide variety of density values, with an average value of $2,800 \pm 250 \text{ kg/m}^3$. There are two areas with different density values: the north area, dominated by the Taburiente edifice, with density values higher than the south part, where is located the volcanic system of Cumbre Vieja, which is the object of study in this work. The high densities to the north of the island could be associated with the materials corresponding to the lifted basal complex [12]. The area is composed by trachytic and phonolitic materials as well as intrusive bodies of a plutonic nature such as gabbros [12]. In Cumbre Vieja Volcano, the density values calculated vary between $2,150\text{-}2,850 \text{ kg/m}^3$ (Figure S2), with an average value of $2,530 \pm 130 \text{ kg/m}^3$. The mean value of the terrain density used to calculate the Bouguer maps of the islands of the Canarian Archipelago is of $2,460 \pm 110 \text{ kg/m}^3$ (Table S4). As we have mentioned below, the average bulk density value of the samples collected for this work is of $2,412 \pm 180 \text{ kg/m}^3$ (Table S5). Combining all this information, a density value of about $2,450 \text{ kg/m}^3$ seems appropriate and representative for the Cumbre Vieja area (Figure S2).

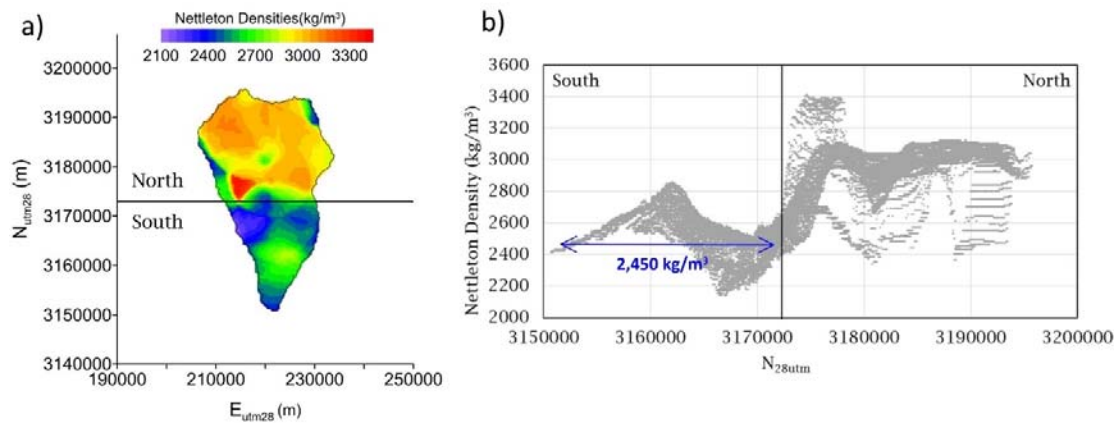


Figure S2. a) Map showing of the distribution of the density values calculated every 100 m according to the Nettleton's method in La Palma Island, seeking the minimum correlation between gravity anomalies and topographic heights. b) Density values plotted vs the N coordinate (28UTM). The black line indicates the sharp change of the density values observed between the north and south areas of the island. A density value of 2,450 kg/m³ is consistent and can be considered as an appropriate mean density to perform the terrain correction.

Table S4. Density values used in several studies to calculate the terrain correction in the Canary Islands archipelago [16, 85, 86, 7, 41, 87, 75, 88, 40].

Island	Terrain density Value	Reference
Fuerteventura	2,500 kg/m ³	Montesinos et al., 2005 [16]
Lanzarote	2,480 kg/m ³	Camacho et al., 2001 [85]
Gran Canaria	2,300 kg/m ³	Camacho et al., 2000 [86]
	2,600 kg/m ³	Montesinos et al., 2022 [7]
Tenerife	2,500 kg/m ³	Sainz-Maza et al., 2019 [41]
El Hierro	2,470 kg/m ³	Montesinos et al., 2006 [87]
	2,510 kg/m ³	Sainz-Maza et al., 2017 [75]
La Gomera	2,560 kg/m ³	Montesinos et al., 2011 [88]
La Palma	2,300 kg/m ³	Camacho et al., 2009 [40]

S4. Covariance analysis to identify the regional gravity component

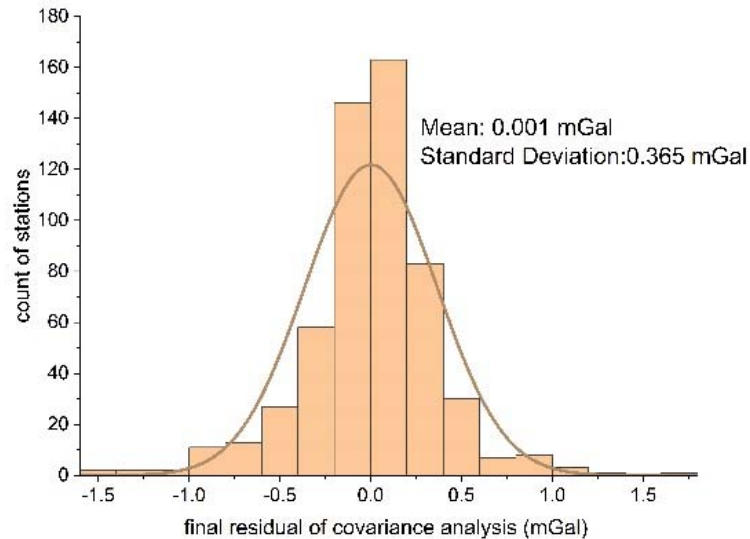


Figure S3. Histogram of the final residuals of the covariance analysis. These residuals are related to the non-correlated noise in the gravity map (Figure 4 in the text).

S5. Energy spectrum analysis of the gravity data

Spector and Grant [89] proposed a statistical technique that involves computing the energy density of the observed data based on the ensemble average of the random distribution of anomalous sources below the plane of observation. These authors observed that when plotting the natural logarithm of the energy of the anomaly versus angular frequency, there is a decay in energy produced by increasing the angular frequency. Syberg [44] mathematically proved that the decay process is mainly controlled by the ensemble average depth of the random distribution of sources, which can be approximated by straight lines (e.g., corresponding to regional/deep and residual/local anomalies). Therefore, the power spectrum can be expressed in terms of straight-line segments, and the slope of each straight line can be converted to the average mean depth of the causative source..

The approach used involved performing a 2D Fast Fourier Transform (FFT) algorithm over the study area to plot the logarithm of the energy of anomalies versus angular radial frequency. The results are displayed in Figure S4 which shows two different sources (h1 and h2) located at mean depths of 11.75 ± 0.7 km and 2.16 ± 0.2 km, respectively. The linear fit for each source has been computed for a 95% confidence interval (blue areas). The deepest source (h1) agrees well with the mean Moho depth obtained for La Palma Island from previous seismic studies [90], and has thus been associated with the crust-mantle interface. The shallower source (h2) represents a density contrast located at a mean depth that can be linked to both the depth of the marine sediments and the mean depth of the submarine volcanic edifice below the island.

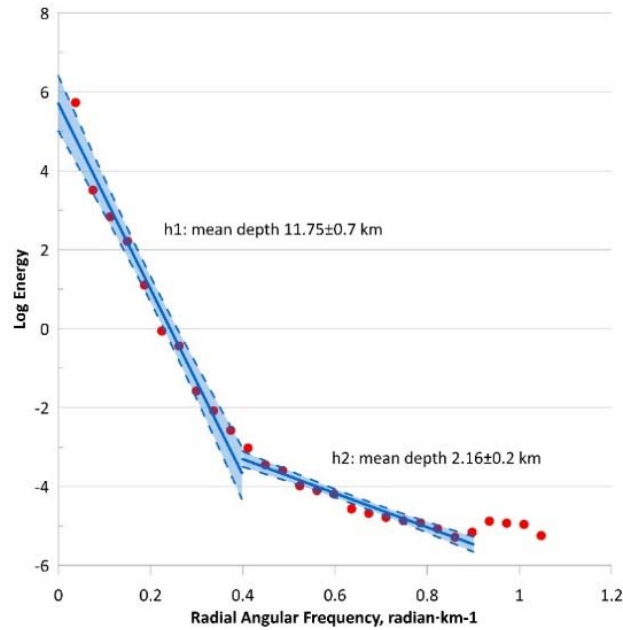


Figure S4. Logarithm of the power spectrum of the Bouguer anomaly vs. the angular radial frequency. Two different linear segments are inferred. These correspond to causative sources located at mean depths of ~ 11.75 km, and ~ 2.2 km. The blue areas represent the 95% confidence interval for the computation of the linear fit.

S6. Gravitational effect of the new topography on the gravity data

The 2021 volcanic eruption in La Palma resulted in a modification of the topography of the island, with an estimated volume of $34 \times 10^6 \text{ m}^3$ [19] of new material covering an area of $\sim 12 \text{ km}^2$. In the most extreme case, some areas experienced a change of elevation up to 200 m, filled with new material. This new excess of mass over the surface modified the gravity field, producing distinguishable changes. The corresponding gravity variations depend on the density of the erupted products and the distance from this new material to the observing point. Aiming to compare with data prior to the eruption, it is possible to model the gravity attraction of this new topography using the same method as for the terrain correction. We used data from the COPERNICUS satellite program (<https://www.copernicus.eu>) to obtain a digital elevation model for the new topography in this study. The volcanic products (lava flows, cones, etc.) were modelled as regular prisms with a $5 \times 5 \text{ m}^2$ base and a height equal to the thickness of the new ground layer. Using the Nagy formula to calculate the gravity attraction of a prism [39], we evaluated the effect on the gravity values of the new topography in each point of the island, every 100 m. The mean density used for the calculation was $3,000 \text{ kg/m}^3$. This value is supported by the grain density of the rock samples from the area during the eruptive process, which have a mean density value of $3,035 \pm 51 \text{ kg/m}^3$ (Table S5). These samples were collected in several locations at the eruption area (Table S5 and Figure S5). This density value is different from $2,450 \text{ kg/m}^3$, which was obtained for the terrain correction using the Nettleton's method. This value represents an average value of the topographic masses of the complete Cumbre Vieja area corresponding to the successive lava flows and pyroclastic products. Therefore, it could be related to the density of the lava flows by considering their porosity (representative of the most scoriaceous part). In this case, the value of the samples is $2,412 \text{ kg/m}^3$, which is similar to the one selected for the global terrain correction. Thus, the grain density samples (it means, without porosity) are more likely to represent the

density of the new lava flows, while the bulk density defines the shallower crustal properties in a more consistent way.

Figure S5 displays the calculated effect of the new topography on the gravity values according to the position of the station. Obviously, the highest calculated effect is below the lavas, where gravity measurements are unable, and it has a value of ~ -10 mGal. In the area where was possible to repeat the measurements, the maximum effect is to 0.15 mGal. According to the calculated gravitational effect of the new topography, the maximum values are located to the east of the main eruptive centre. Based on this model, it is possible to subtract the gravity contribution of this effect from the January 2022 gravity data and to compare them with the corresponding ones of July 2021. Once the free air effect (FAC) due to the vertical displacement of the ground and the influence of this new topography are removed, it can be expected that gravity differences are mainly due to the subsurface mass redistribution as a consequence of the eruptive process.

Table S5. Bulk and grain density values obtained from basanitic and tephritic lava flows of the 2021 eruption at Cumbre Vieja.

Sample	Bulk density (kg/m³)	Grain density (kg/m³)
LP0	2251.3	2926.5
LP1	2228.6	3055.9
LP2	2581.4	3067.9
LP3	2667.1	3067.0
LP4	2219.4	2942.7
LP5	2204.5	3070.1
LP6	2421.8	3047.2
LP7	2303.1	3043.7
LP8	2427.2	3040.4
LP10	2603.7	3067.4
LP11	2625.4	3061.8
Mean	2412.1	3035.5
Standard deviation	181.1	51.1

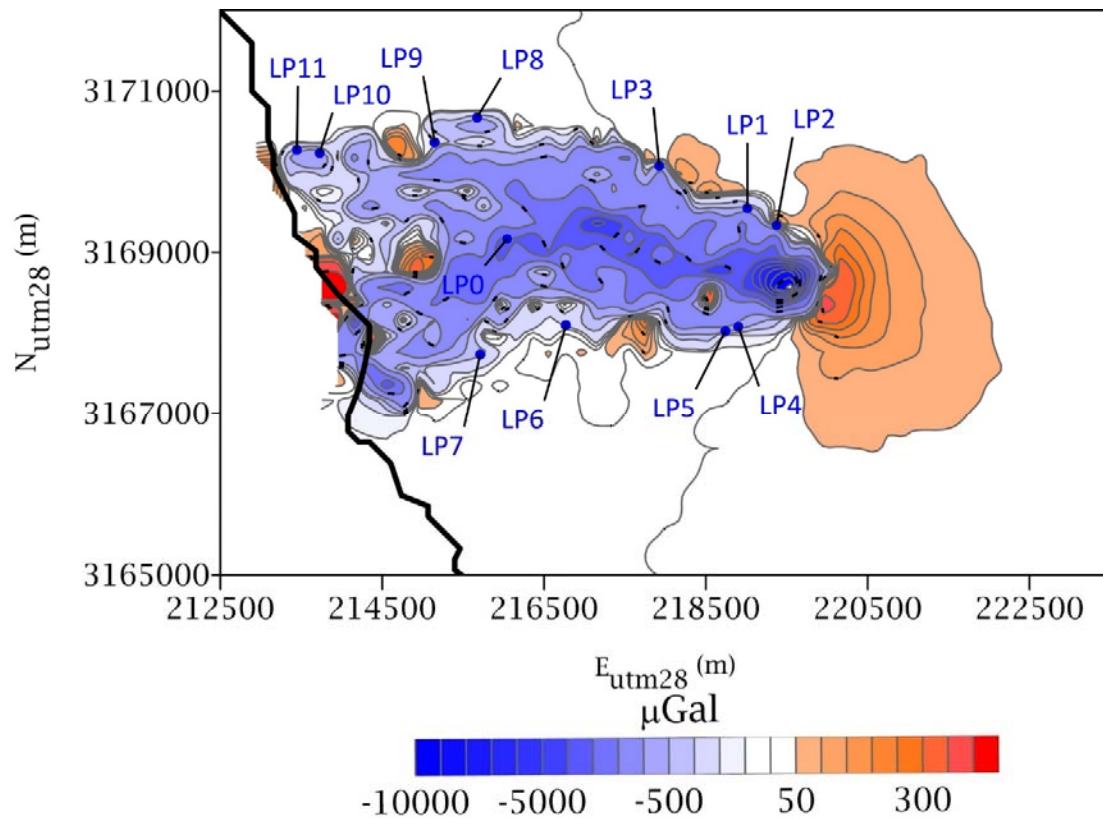


Figure S5. Gravity effect induced by the new topography as a consequence of the 2021 eruption in Cumbre Vieja. The effect is calculated over the terrain model before the eruption. The density used for the lava flows is $3,000 \text{ kg/m}^3$. The labels LP0 to LP11 indicate the location of the samples of bulk and grain density values obtained from basanitic and tephritic lava flows (Table S5).

S7. Gravity Inversion model

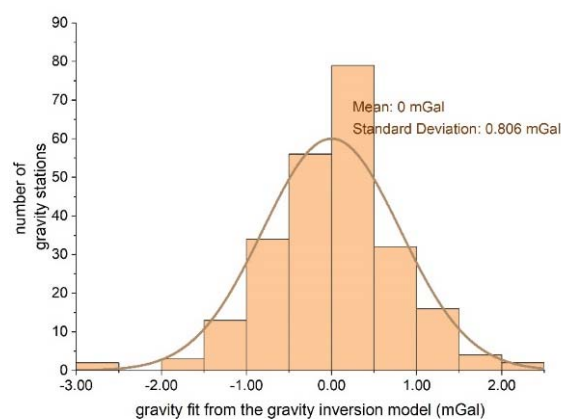


Figure S6. Histogram of the fit between the local gravity data (Figure 5b in the paper) and the calculated gravity from the inversion model obtained using the genetic algorithm [30].

S8. Estimation of the width of the feeder dyke and related sills from aspect ratio analysis

The aspect ratio is the length-thickness ratio of a feeder-dyke or a volcanic fissure. Gudmundsson [49, 50] developed a method that using elastic fracture mechanics and overpressure estimates for magma-filled fractures, relates the opening of an elastic mode I (tensile mode) crack as a function of its constant internal fluid overpressure (1):

$$\Delta u_I = \frac{2p_0(1-\nu^2)L}{E} \quad (1)$$

where Δu_I represents the maximum (central) opening displacement of a volcanic fissure, p_0 is the internal fluid overpressure, ν is the Poisson's ratio, L is the smaller of the strike and dip dimensions of the fracture, and E is the Young's module. For a feeder-dyke connecting the magma chamber with the surface, L is smaller (or roughly equal to) the dip-dimension of the dyke.

Gudmundsson [49] established that the overpressure of the dyke at the surface is given by:

$$p_0 = p_e + (\rho_r - \rho_m)gh + \sigma_d \quad (2)$$

where p_e is the fluid excess pressure in the source magma chamber, ρ_r is the average rock density, ρ_m is the average magma density, g is the gravity acceleration, h is the depth to the magma chamber and σ_d is the differential stress at the surface.

By combining equations (1) and (2), the depth to the intersection between the feeder-dyke and the magma chamber can be expressed by the equation 3:

$$h = \frac{\Delta u_I E}{2L(1-\nu^2)(\rho_r - \rho_m)g} - \frac{p_e + \sigma_d}{(\rho_r - \rho_m)g} \quad (3)$$

This equation is commonly used to estimate the depth of the source magma chamber from measurements of the maximum dyke aperture visible at the field, where the erosion or the geological conditions allows to be directly measured (e.g., Iceland and Tenerife, [83]; El Hierro, [45]). However, this equation can also be used to obtain an estimation of the maximum dyke aperture if the depth of the source magma chamber is known. This is the case of the Cumbre Vieja eruption, where the location of the volcano-tectonics (VT) events associated to the initiation and development of the feeder-dyke provide a good estimation of the parameters needed to compute the maximum aperture of the dyke causing the eruption.

In Figure S1, the pre-eruptive seismicity reveals a clear upwards propagation of the hypocentres of the VT events from September 11th to 19th. The deeper events were located at 8-10 km b.s.l., so this is the estimated depth to the roof of the source magma chamber (h in equation 3). Moreover, the projection of the hypocentral locations, as the VT events propagated upwards, define a $\sim 60^\circ$ SE plunge line with a $\sim 1-2$ km width with respect to the VT propagating front. Once the eruption started, several aligned vents trending NW-SE were observed. The total distance between the vents along the fissure eruption is $\sim 1-1.5$ km (not all the vents were active at the same time during the eruptive process) that could be used as a good proxy to the strike length of the feeder-dyke [50]. Considering both the geological and seismic data, 1 km seems to be a reasonable value for the strike dimension (L) of the feeder-dyke.

The density values can be determined from typical basaltic magma ($2,650 \text{ kg/m}^3$) and oceanic crust ($2,800 \text{ kg/m}^3$) (e.g., [57, 91, 80]). La Palma is a volcanic island developed on Jurassic oceanic crust, and Cumbre Vieja area is composed by gabbroic plutonic rocks, basaltic lava flows and dykes, and mafic pyroclastic layers (see Introduction section in the main text). Therefore, a mean value of $2,800 \text{ kg/m}^3$ is representative of the oceanic crustal segment where the dyke has been emplaced.

Regarding the fluid excess pressure (p_e), it represents the difference between the pressure in the magma chamber at the moment of the rupture and the lithostatic pressure. The initiation of the feeder-dyke occurs where the fluid excess pressure reaches the tensile strength, which commonly is in the range of 0.5-9 MPa but the more typical in-situ tensile strength value ranges from 2.5-4 MPa [80, 91-93]. As previously described, σ_d is the difference between the vertical stress and the minimum principal horizontal stress (σ_3) at the surface (i.e., at the point of initiation of the volcanic fissure). As the vertical stress at the surface corresponds to the atmospheric pressure, the value of σ_d corresponds to the in-situ tensile stress of the surface layer. The materials outcropping at the location of the Cumbre Vieja volcano are basaltic lava flows and mafic pyroclastics layers, so a mean representative value for σ_d would be 1 MPa [92, 93]. Finally, typical values for similar volcanic areas of 5 GPa and 0.25 for Young's modulus and Poisson's ratio respectively have been used [49, 50, 56].

Using all the previous parameters in equations 1-3 and considering a 10% uncertainty in the determination of the geometric dimensions, the maximum opening displacement of the volcanic fissure Δu_l associated to the Cumbre Vieja volcano would be of 6.7 ± 1.5 m. This value is similar to that found in previous studies of feeder-dykes in similar volcanic areas, such as Iceland, Tenerife and El Hierro [56, 50, 57]. Using the inferred lateral dimensions of the sills, similar computations can be used to provide maximum aperture thicknesses of 11.0 ± 2.2 m, 5.9 ± 1.1 m, 4.4 ± 0.9 m and 5 ± 0.9 m for the sills located at depths of 12 km, 6 km, 2 km and 1 km, respectively.

Considering the maximum opening value obtained, the total volume along the whole magma plumbing system would be approximately of $217 \cdot 10^6$ m³, which is similar to that of the total estimates of the erupted material [94].

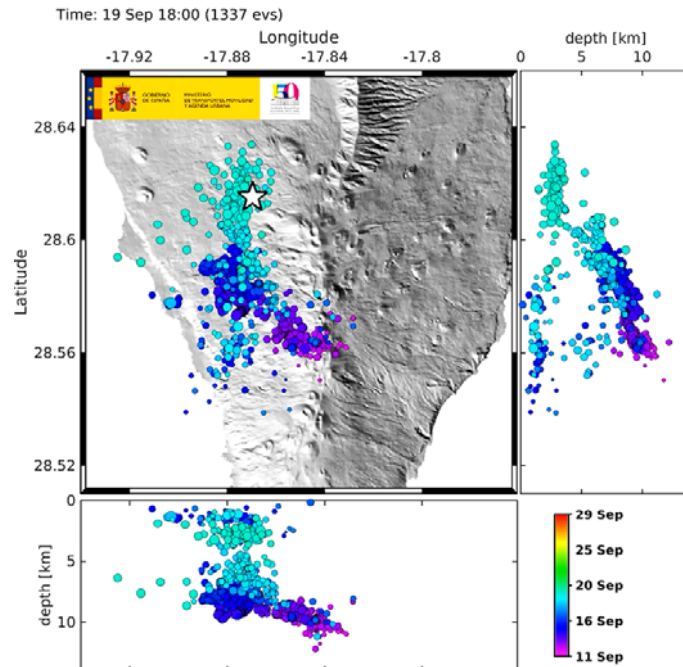


Figure S7. Location of the VT events corresponding to the pre-eruptive stage (up to September 19th). The white star marks the location of the eruptive vent. Data source: Spanish Geographic Institute, <https://www.ign.es/web/ign/portal/sis-catalogo-terremotos>.

S9. Model of the magma plumbing system for the 2021 eruption of Cumbre Vieja volcano

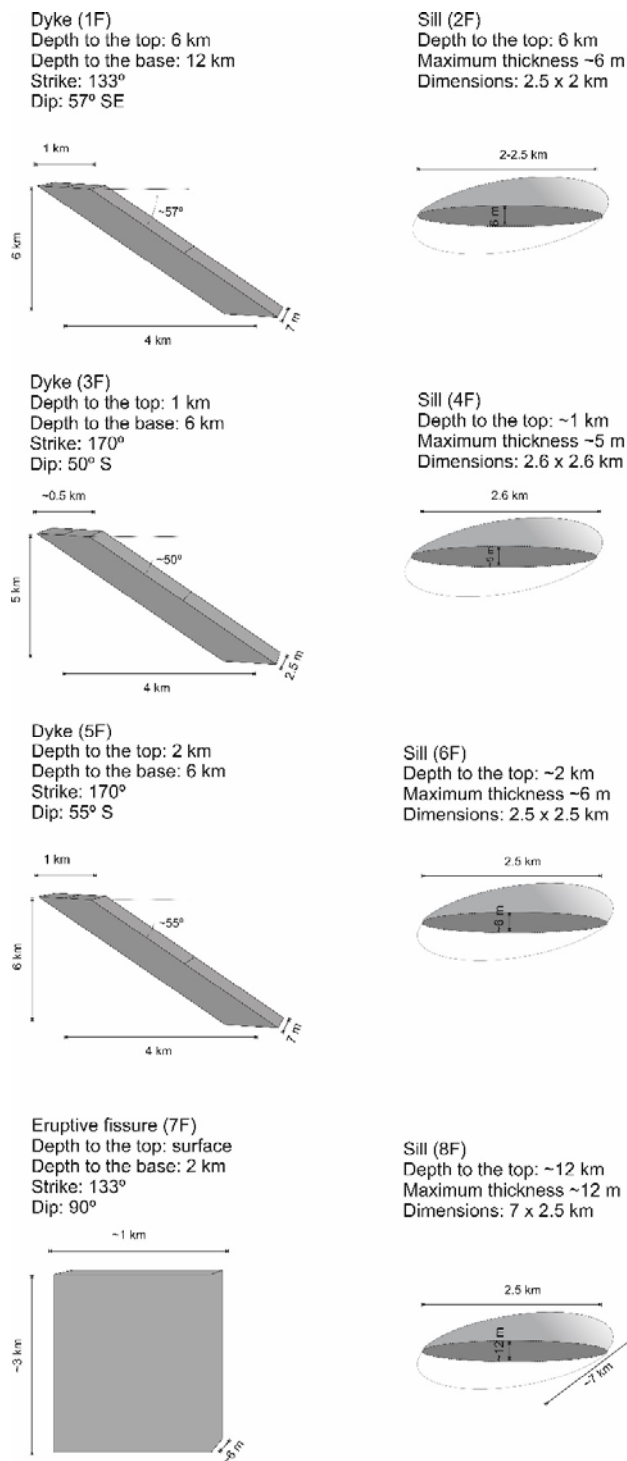


Figure S8. Geometric characteristics of the 8 simple bodies (dykes and sills) constituting the elements of the simple magma plumbing system model.

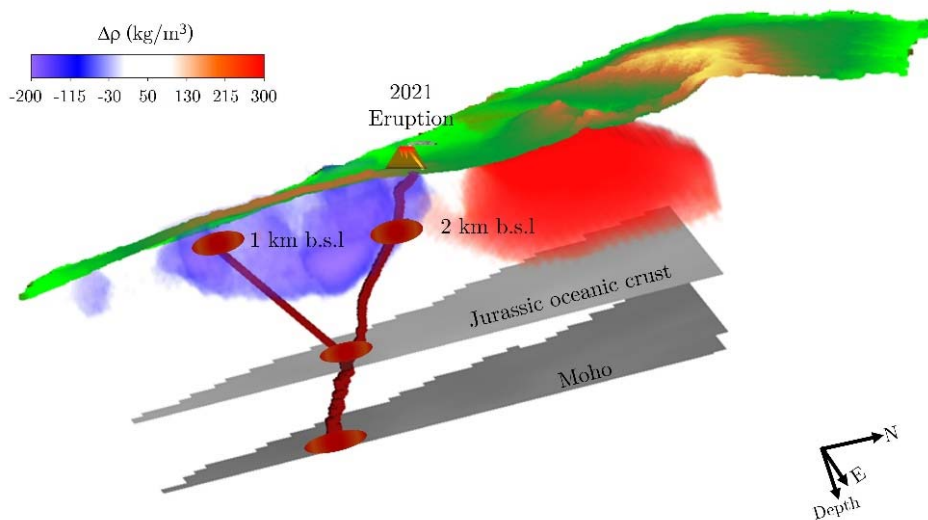


Figure S9. Conceptual model (view from the SE) of the inferred magma system obtained from the forward modelling using the dykes and sills shown in Figure S8. The density contrast structures calculated from the inversion of gravity data are displayed in red-blue colour scale. Ascending dykes (brown paths) are turned into sills (brown ellipses) that are located where different structural limits are identified. The low density structure handles the final path for the dykes, supporting the hypothesis of the model of magmatic plumbing system proposed.

Data Set S1. File: GravityCumbreVieja_FGMontesinos_et_al.dat

The gravity data are provided as supplementary data for the peer-review purpose. Upon acceptance, this file will be available for the readers from the Zenodo repository (doi:10.5281/zenodo.7539248).

The file GravityCumbreVieja_FGMontesinos_et_al.dat includes the values of gravity and complete Bouguer gravity anomaly (GRS80) calculated for the land gravity stations at the Cumbre Vieja area (La Palma Island, Spain). The gravity values were observed in 142 land gravity stations (Figure 3 in the manuscript) by our group in 2005 and 2021 surveys. The positions of the stations were selected to cover most of the Cumbre Vieja area, and the coordinates were obtained by differential GPS (WGS84 Datum). The gravity observations were processed considering the usual corrections (instrument height, drift, jumps, etc.). The tidal correction was calculated from gravity tide measurements made in several islands of the Canary Archipelago. All the gravity values are referred to the absolute gravity stations (Table S1). The procedure to obtain the terrain correction and the Bouguer anomaly map is explained in the manuscript and in the supporting information.

Data Set S2. File: GravityNETWORKCumbreVieja_FGMontesinos_et_al.dat

The gravity change values in the network observed between July 2021 and January 2022 (project PID2019-104726GB-I00/AEI/10.13039/501100011033) are provided as supplementary data for the peer-review purpose. Upon acceptance, this dataset will be available from the Zenodo repository (<https://doi.org/doi:10.5281/zenodo.7570284>). The file contains gravity and height differences between both surveys achieved during 2021 and 2022. From this data set, the free air correction with a gradient of $-308.6 \mu\text{Gal/m}$ and a correction of the attraction effect of the new topography on the gravity data are applied. The final residual gravity changes between both surveys are shown with the corresponding error.